ARTICLE IN PRESS
YNIMG-05469; No. of pages: 9; 4C: 4, 5, 6, 7
NeuroImage xxx (2008) xxx-xxx
Contents lists available at ScienceDirect
NeuroImage
journal homepage: www.elsevier.com/locate/ynimg

Integration of motion correction and physiological noise regression in fMRI

Tyler B. Jones, Peter A. Bandettini, and Rasmus M. Birn*

Laboratory of Brain and Cognition, National Institute of Mental Health, NIH, Bethesda, MD, USA

ARTICLE INFO

Article history:
Received 26 February 2008
Revised 28 April 2008
Accepted 7 May 2008
Available online xxxx

ABSTRACT

Physiological fluctuations resulting from the heart beat and respiration are a dominant source of noise in fMRI, particularly at high field strengths. Commonly used physiological noise correction techniques, such as RETROspective Image CORrection (RETROICOR), rely critically on the timing of the image acquisition relative to the heart beat, but do not account for the effects of subject motion. Such motion affects the fluctuation amplitude, yet volume registration can distort the timing information. In this study, we aimed to systematically determine the optimal order of volume registration, slice-time correction and RETROICOR in their traditional forms. In addition, we evaluate the sensitivity of RETROICOR to timing errors introduced by the slice acquisition, and we develop a new method of accounting for timing errors introduced by volume registration into physiological correction (motion-modified RETROICOR). Both simulation and resting data indicate that the temporal standard deviation is reduced most by performing volume registration before RETROICOR and slice-time correction after RETROCIOR. While simulations indicate that physiological noise correction with regressors constructed on a slice-by-slice basis more accurately modeled physiological noise compared to using the same regressors for the entire volume, the difference between these regression techniques in subject data was minimal. The motion-modified RETROICOR showed marked improvement in simulations with varying amounts of subject motion, reducing the temporal standard deviation by up to 36% over the traditional RETROICOR. Though to a lesser degree than in simulation, the motion-modified RETROICOR performed better in nearly every voxel in the brain in both high- and low-resolution subject data.

Introduction

Physiological fluctuations resulting from the heart beat and respiration are a dominant source of noise in Blood Oxygenation Level Dependent (BOLD) fMRI, particularly at high field strengths (Kruger and Glover, 2001). Cardiac, respiratory and other low-frequency noise is particularly prominent in grey matter (GM), the region of primary interest in most fMRI studies (Dagli et al., 1999; Kruger and Glover, 2001; Weisskoff et al., 1993; Wise et al., 2004). This physiological noise increases signal variance, effectively decreasing signal detection power. In addition, the structured nature of this noise compromises the independent and identically distributed (i.i.d.) statistical assumption made of the noise in most fMRI data analysis (Lund et al., 2006). Beyond traditional activation paradigms, physiological noise is particularly confounding in connectivity studies which infer connections between brain areas based on the temporal correlation of fluctuations in the time series of anatomically remote regions (Birn et al., 2006; Biswal et al., 1995; Cordes et al., 2000; Lowe et al., 1998; Lund, 2001). Therefore, it is advantageous to account for errors introduced by physiological fluctuations in most applications of fMRI.

A commonly used physiological correction technique currently applied to fMRI data is RETROspective Image CORrection (RETROICOR) (Glover et al., 2000). RETROICOR models the cardiac and respiratory fluctuations using a Fourier series defined by the phase relative to the cardiac and respiratory cycles, respectively, at the time of image acquisition (Eqs. (1), (2) and (3)). The phase of the cardiac cycle, ϕ_c, is defined by the time to the nearest preceding heart beat divided by the time between the heart beats (the cardiac period); the phase of the respiratory cycle, ϕ_r, is defined by the depth of the breath at the time of the image acquisition relative to a histogram (scaled from 1 to 100) of the respiration depth across the entire imaging run.

$$y_{c/r}(x,t) = \sum_{m=1}^{M} a_{c/r}(x)\cos\left(m\phi_{c/r}(t)\right) + b_{c/r}(x)\sin\left(m\phi_{c/r}(t)\right) \quad (1)$$

$$\phi_c(t) = 2\pi(t-t_1)/(t_2-t_1) \quad (2)$$

$$\phi_r(t) = \pi\frac{\sum_{b=1}^{100\cdot rnd[R(t)/R_{max}]} H(b)}{\sum_1^{100} H(b)} \quad (3)$$

* Corresponding author. Laboratory of Brain and Cognition, National Institute of Mental Health, 10 Center Dr., Bldg 10, Rm 1D80, Bethesda, MD 20892-1148, USA. Fax: +1 301 402 1370.
E-mail address: rbirn@nih.gov (R.M. Birn).
Available online on ScienceDirect (www.sciencedirect.com).

1053-8119/$ – see front matter © 2008 Published by Elsevier Inc.
doi:10.1016/j.neuroimage.2008.05.019

In Eqs. (1) and (2), $y_{c/r}(x,t)$ is the cardiac or respiratory (c/r) induced signal fluctuation, $\phi_{c/r}(t)$ is the phase of the cardiac or respiratory cycle at the time of image acquisition, M is the Fourier fit order, $a_{c/r}$ and $b_{c/r}$ are Fourier fit coefficients determined in the regression analysis, t is the time of image acquisition, t_1 is the time of the preceding heart beat, and t_2 is the time of the following heart beat. In Eq. (3), $R(t)$ is the respiration depth, Rmax is the maximum depth of respiration, and $H(b)$ is the histogram of respiration depth over the entire imaging run. For more details see Glover et al. (2000). The RETROICOR method has been shown to be effective in minimizing the spectral bands associated with respiratory and cardiac artifacts, even when aliasing occurs due to non-critical sampling. However, this method does not account for the effects of subject motion.

Physiological correction techniques, such as RETROICOR, rely critically on the timing of the image acquisition relative to the heart beat. During a typical interleaved slice-acquisition scheme, neighboring slices may be acquired up to several seconds apart, depending on repetition time (TR). Because of this, RETROICOR should ideally be performed on a slice-by-slice basis (Birn et al., 2006). Subject motion, however, can cause additional problems. Prior to volume registration, the signal intensity in a voxel can change substantially due to the motion of the brain relative to the imaged voxel. In addition, cardiac fluctuations present in a particular brain area can move from one voxel to another. A particular voxel may therefore contain the fluctuations for only parts of the imaging run, which is not modeled well by a Fourier series. Volume registration, on the other hand, will result in voxels containing a mixture of signals acquired at different times. The traditional RETROICOR regressors do not account for this mixture of timing information.

The difference in acquisition times of different slices is typically corrected by interpolating the imaging time series in each slice to a common time grid. This "slice-time correction" step, for example, is particularly important for event related tasks where accurate timing of stimulus onset is critical for activation detection. However, this method does not account for "mixing" of slice-acquisition times after volume registration. Additionally, up to three heart beats can occur in a typical whole-brain functional TR of ~2 s. Interpolating the data point to a time occurring seconds earlier, therefore, will not accurately reflect the phase of the cardiac cycle in which the image was actually acquired. This would effectively corrupt the cardiac timing information, limiting RETROICOR's ability to remove cardiac fluctuations. Furthermore, applying slice-time correction to data containing aliased cardiac noise may lead to erroneous signal intensity changes, again suggesting that this step should be performed after RETROICOR. Respiration fluctuations would be less severely corrupted by slice-time correction because their frequency is typically much lower than the Nyquist frequency of the image acquisition rate (determined by the TR).

The main goals of the current study are three-fold. We aimed to systematically determine the optimal order of volume registration, slice-time correction and RETROICOR in their traditional forms. Additionally, we evaluated the sensitivity of RETROICOR to errors in the model introduced by the slice-acquisition timing. Lastly, we investigated a new method of incorporating estimated motion correction parameters into physiological correction, accounting for timing errors introduced by volume registration.

Methods

Optimal order of traditional corrections

The optimal order of corrections was first analyzed in a simulated dataset. In order to simulate the acquisition of slices at different times, we began by creating a baseline time series of image volumes with a temporal resolution finer than the imaging TR (3 s). This baseline was created by taking a single functional image volume from in-vivo data, and copying this volume 1760 (80*22=the number of image volumes*the number of slices) times, thus creating a constant baseline time course in every voxel. The time series had an effective time step of 0.136 s (3 s/22=repetition time/number of slices) corresponding to the time between slice acquisitions. After creating a baseline time series of image volumes at this fine temporal resolution, sinusoidal fluctuations of constant amplitude at a frequency of 1.1 Hz mimicking cardiac fluctuations were added to voxels that showed the highest variance in subject data (~~GM and CSF~~), areas also expected to have the largest physiological noise component. Motion was then applied to the dataset using the six rigid-body realignment parameters estimated from volume registration for the same subject as was used to create the baseline. These realignment parameter time series were extended to the finer slice-acquisition time grid by assuming that the motion occurred only between the acquisition of full volumes (i.e. on integer–TR intervals, once every 3 s). The volumes were then re-sliced in order to simulate the 2-dimensional slice-by-slice image acquisition. This procedure involved sub-sampling the high temporal resolution dataset according to when each slice would have been acquired in the interleaved acquisition (i.e., the first slice was taken from the first volume in the high temporal resolution dataset, the second slice was taken from the second volume, etc.). In sum, the simulation created a series of image volumes at a finer temporal resolution, which could be moved (rotated and translated) according to simulated subject motion and then re-sliced to simulate the slice acquisition. Other parameters were identical to the high-resolution scans from subject data evaluated and described below: 128×128 resolution, TR/TE=3000 ms/30 ms, 80 images per run, 24 cm FOV, 22 5 mm thick slices and axial interleaved acquisition. All orders of volume registration (3dvolreg), RETROICOR, and slice-time correction (3dTshift) were then applied to the dataset. The temporal standard deviation was calculated in every voxel and averaged over voxels in which the original fluctuations were added (GM, CSF, and large vessels). Correction efficacy was defined as the percent decrease of temporal noise after correction, or the difference in the average standard deviation between the corrected and uncorrected datasets divided by the standard deviation of the uncorrected dataset times 100. This analysis was repeated with various levels of random Gaussian-distributed white-noise added to the baseline. All simulations and data analysis was performed in AFNI (Cox, 1996).

The order of corrections was also analyzed in fourteen resting-state subject datasets. Gradient Echo EPI data were recorded from all subjects on a 3 T General Electric (GE) Signa MR scanner (Waukesha, WI). Ten subjects were acquired with a 64×64 resolution, TR/TE=2000 ms/30 ms, 165 images per run, 24 cm FOV, 27 5 mm thick slices and sagittal interleaved acquisition. Four subjects were acquired with 128×128 resolution, TR/TE=3000 ms/30 ms, 80 images per run, 24 cm FOV, 22 5 mm thick slices and axial interleaved acquisition.

Please cite this article as: Jones, T.B., et al., Integration of motion correction and physiological noise regression in fMRI, NeuroImage (2008), doi:10.1016/j.neuroimage.2008.05.019

Physiology was recorded with a finger-clipped pulse oximeter and pneumatic respiration belt wrapped around the chest at the level of the diaphragm. The physiological recording devices were provided by the scanner manufacturer (GE), integrated into the MRI scanner, and synchronized with the scan acquisition. Cardiac and respiratory data was written into a text file on the MR console with a sample every 25 ms.

The individual subject values for the standard deviation reduction were calculated as the average value across all voxels in the brain for the low-resolution datasets and the average value across voxels in GM, cerebrospinal fluid (CSF) and large vessels in the high-resolution subjects where venograms and tissue segmentation maps were available.

Sensitivity of RETROICOR to timing errors introduced by the slice acquisition

The original application of the RETROICOR method constructed Fourier regressors based on the timing information of the entire volume (Glover et al., 2000). One could also construct these regressors for every slice independently since the timing information for each slice is known. From here on out we will refer to RETROICOR with the same regressors for every slice as the "phase-locked" version and with separate regressors for every slice as the "slice-specific" version.

We first performed a simulation to determine the sensitivity of RETROICOR to an offset of the timing between the image acquisition and the heart beat. A simple sine wave with variable frequency (mimicking natural fluctuations in cardiac rate) was used as a known input. This sine wave was sub-sampled to the imaging TR. The RETROICOR correction was performed on this sub-sampled dataset, using the phase of the cardiac cycle at which either 1) each slice was acquired (the "slice-specific" version) or 2) the first slice was acquired (the "phase-locked" version). This simulation was repeated for different levels of cardiac variability, i.e. cardiac period standard deviations ranging from 0 to 0.2 s. In this simulation, the standard deviation of the residuals was computed and used as a measure of RETROICOR's ability to model the physiological signal.

RETROICOR robustness was also evaluated in subject data. The same ten low-resolution subject datasets were used as for the order of corrections analysis. Both the phase-locked and slice-specific versions of RETROICOR were applied after volume registration.

Motion-modified RETROICOR

RETROICOR was modified to take slice timing errors introduced by registration into account. The traditional Fourier regressors specific to each slice were replaced by a new set of Fourier regressors specific to each voxel. These new regressors retained the slice timing information and were scaled by a slice contribution factor, $w_{nz}(x,t)$, which represents the proportion that each slice contributes to a particular voxel, x, at a certain time, t (Eq. (4)). This slice contribution was calculated by applying the estimated subject motion to a dataset that consisted of the value 1 everywhere in a particular slice and 0 in all other slices. The spatial interpolation involved in the translation and rotation changed this value of 1 to a value between 0 and 1, which reflects the proportion that the particular slice contributed to each voxel at a given point in time. This computation was performed for each slice.

$$y_c(x,t) = \sum_{m=1}^{M} \sum_{nz=0}^{NZ} w_{nz}(x,t)[a_{c,nz}(x)\cos(m\phi_c(t)) + b_{c,nz}(x)\sin(m\phi_c(t)). \quad (4)$$

In Eq. (4), $y_c(x,t)$ is the cardiac-induced signal fluctuation, $\phi_{cnz}(t)$ is the phase of the cardiac cycle at the time of slice nz acquisition, $w_{nz}(x,t)$ is the proportion that each pre-registered slice contributed to every voxel and time point after registration (the slice contribution), NZ is the number of slices, M is the Fourier fit order, and $a_{c,nz}$ and $b_{c,nz}$ are Fourier fit coefficients determined in the regression analysis. Note that in this model, for every regressor with increasing amplitude, there was a corresponding regressor, or linear combination of regressors, with decreasing amplitude, modeling fluctuations moving into versus out of a voxel of interest, respectively.

This analysis is likely to be considerably slower than a typical multiple regression analysis, since it requires a separate set of regressors for each voxel, as well as a computation of the slice contributions to each voxel, as described above. One could consider the contributions of any slice to a given voxel, however, this would require 120 regressors for a dataset with 30 slices (4 sinusoidal regressors * the number of slices). In order to speed up the computation of slice contributions and reduce the number of regressors, only the contributions from neighboring slices were considered. Voxels that are two slices away were acquired only about 100 ms before or after the slice in question in an interleaved acquisition (assuming a 3 s TR, 30 slices, and evenly spaced slice acquisitions throughout the TR interval). For a slice thickness of 4 mm, contributions from voxels that are 3 slices away would require a significant amount of movement (a translation of 12 mm or more; or a rotation of greater than 3.4°, assuming a 20 cm FOV and rotation around a fulcrum at the edge of the image). At that amount of movement, other factors such as spin-history effects or B_0-field distortions are likely to play more significant roles.

The motion-modified RETROICOR technique was applied to resting-state data from two subjects that showed a significant amount of motion (>1.5 mm during the imaging run). Gradient Echo EPI data were recorded from both subjects on a 3 T GE Signa scanner (Waukesha, WI). One subject was acquired with 64×64 resolution, TR/TE=3000 ms/30 ms, 110 images per run, 24 cm FOV, 5 mm slice thickness and axial interleaved slice acquisition. The other subject was acquired with 128×128 resolution, TR/TE=3000 ms/30 ms, 80 images per run, 24 cm FOV, 5 mm slice thickness and axial interleaved slice acquisition. Physiology was recorded with a finger-clipped pulse oximeter and a pneumatic respiration belt wrapped around the chest at the level of the diaphragm.

To further evaluate the performance of this new motion-modified RETROICOR we performed two simulations. The purpose of the first simulation was to duplicate the conditions (particularly the motion) of the low-resolution subject data. The purpose of the second simulation was to evaluate the effect of increasing amounts of movement on various corrections. In both simulations, the datasets were created in a similar manner as that described previously. A single functional image from the low-resolution subject described above was copied 3300 (110*30=the number of image volumes*the number of slices) times to produce a baseline time course in every voxel. In the first simulation, sinusoidal physiological fluctuations with

Please cite this article as: Jones, T.B., et al., Integration of motion correction and physiological noise regression in fMRI, NeuroImage (2008), doi:10.1016/j.neuroimage.2008.05.019

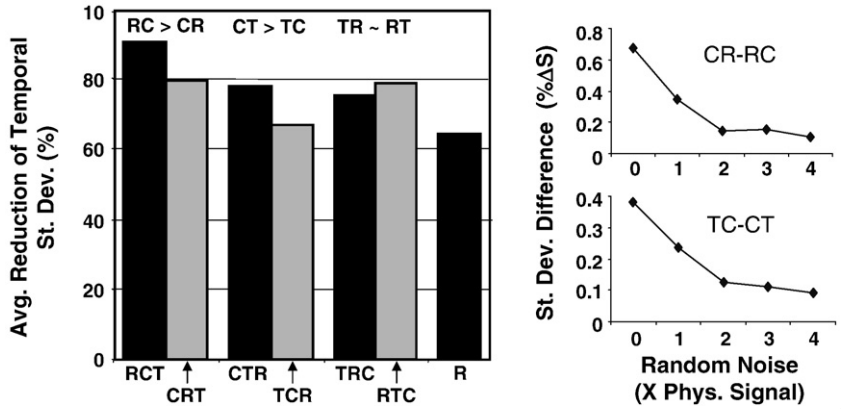

Fig. 1. Noise reduction for the orders of different corrections in simulated data with added sinusoidal physiological fluctuations in grey matter (GM), CSF and large vessels, and simulated subject motion. Volumetric and motion parameters were taken from high-resolution subject data. The average reduction of temporal standard deviation represents the percent noise reduction compared to no correction. The plots on right represent the difference of the residual standard deviations after application of the two correction orders (CR–RC, top; TC–CT, bottom) at random noise levels of 0 to 4 times the physiological signal. Abbreviations: Registration (R), RETROICOR (C), slice-time correction (T). The order of letters refers to the temporal sequence of the corrections (e.g. RCT = Registration, followed by RETROICOR, followed by slice-time correction).

amplitude of 2.5% signal change were added to a spherical ROI in the frontal region of the brain — an area known to have significant through-plane movement with axial acquisition. Motion was then applied to this dataset using the same six rigid-body realignment parameters estimated from the volume registration in this low-resolution subject. In the second simulation, sinusoidal physiological fluctuations of amplitude 2.5% signal change were added to a single mid-axial slice (z=15) with the same fluctuation of amplitude 1.125% signal change added to the neighboring slice. A linear translation in the through-plane (axial) direction of varying magnitude from 0 mm to 5 mm occurring during the imaging run was then applied to this dataset. The time series in both simulations were sub-sampled to the imaging TR by selecting one slice, in interleaving order, from each volume, and then assembling these slices into 110 new volumes. Volume registration followed by either the traditional RETROICOR or the motion-modified RETROICOR were then applied to both simulated datasets. For the first simulation, the temporal standard deviation was calculated and averaged over all voxels in the frontal sphere containing physiological fluctuations. For the second simulation, the temporal standard deviation was calculated and averaged over all voxels in slice 15. These average standard deviations were again compared to that of the uncorrected dataset (in terms of percent noise reduction) to give a measure of method efficacy.

Results

Optimal order of traditional corrections

Based on simulations, the optimal order of corrections in terms of temporal standard deviation reduction is first performing volume registration, then applying RETROICOR, followed by slice-time correction (RCT) (Fig. 1). As a basis of comparison, the noise reduction of registration alone is included in Fig. 1. When looking at the order of specific corrections, one can see that it is better to perform registration prior to RETROICOR, and RETROICOR prior to slice-time correction (Fig. 1). Though not the focus of this study, it should also be noted that there is only a marginal difference of the residual standard deviation when the order of registration and slice-time correction is reversed (Fig. 1).

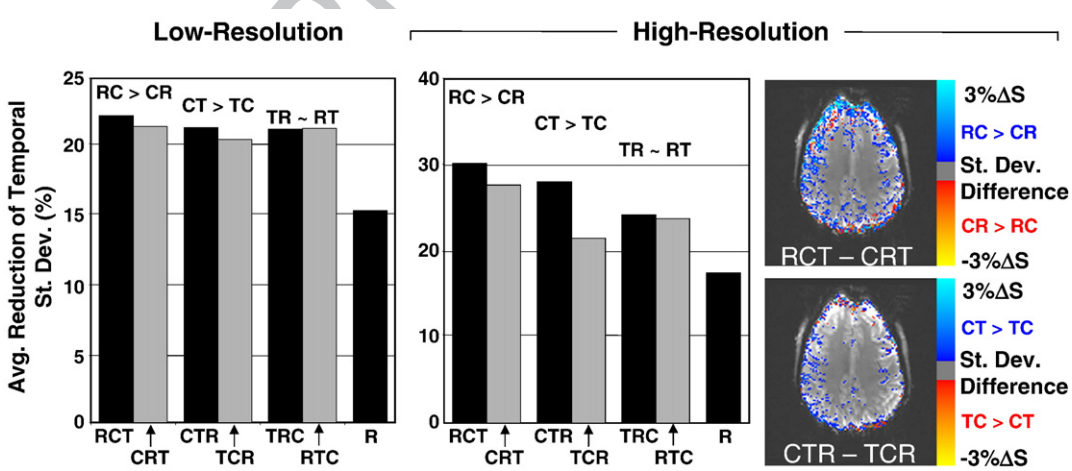

Fig. 2. Noise reduction for the orders of different corrections in subject data. Individual subject values of temporal standard deviation were averaged across the whole brain at low resolution and across only grey matter (GM), CSF and large vessels at high-resolution. The average reduction of temporal standard deviation represents the percent noise reduction compared to no correction averaged across the 10 low-resolution subjects (left) and 4 high-resolution subjects (right). Individual subject values were submitted to two-tailed, paired t-tests, showing 'RCT' as significantly better than all other correction orders both at high and low resolutions ($p<0.05$). The images on the right represent the difference of the residual standard deviations after application of the two correction orders (RCT-CRT, top; CTR-TCR, bottom) in a single subject. Abbreviations: Registration, followed by RETROICOR, followed by slice-time correction).

Please cite this article as: Jones, T.B., et al., Integration of motion correction and physiological noise regression in fMRI, NeuroImage (2008), doi:10.1016/j.neuroimage.2008.05.019

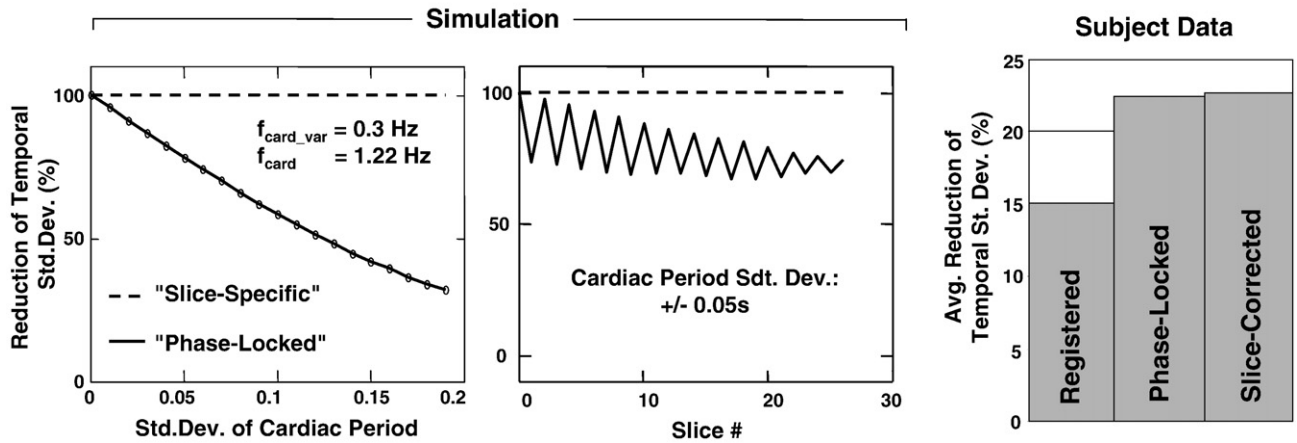

Fig. 3. Sensitivity of RETROICOR to timing errors introduced by the slice acquisition. The reduction of temporal standard deviation represents the percent noise reduction compared to no correction. In subject data (plot on right), individual values of temporal standard deviation reduction were averaged across the whole brain and then across subjects. The difference between the phase-locked and slice-corrected versions of RETROICOR were significant in subject data (two-tailed, paired *t*-test, $p=0.026$).

Similar results were obtained in the 10 low-resolution subjects with sagittal slice acquisition, although the difference is not very large. All correction orders were significantly better than registration alone (two-tailed, paired *t*-test: for all orders $p<0.0001$). Though the difference in the orders was minimal, first performing volume registration, then RETROICOR, followed by slice-time correction (RCT) was the optimal order in eight out of the ten subjects (Fig. 2). The next best correction order on average, RETROICOR, then volume registration, followed by slice-time correction (CRT), was optimal in the other two subjects. Even though there was a large variance in the correction efficacy among the subjects, across the group, RCT was significantly better than all other orders, including CRT (two-tailed, paired *t*-tests: RCT–CRT $p=0.016$, RCT–CTR $p<<0.0001$). In agreement with the simulation, the difference between the order of registration and slice-time correction was not significant (two-tailed, paired *t*-test: RTC–TRC $p=0.062$) (Fig. 2).

Fig. 2 also shows the standard deviation following different orders of correction for the four subjects acquired with axial slices at higher resolution. All four subjects showed RCT as the optimal order with much larger differences between the correction orders than in the low-resolution subjects. This order (RCT) was significantly better than all other orders, including the next best order, RETROICOR, slice-time correction, followed by registration (CTR) (two-tailed, paired *t*-tests: RCT–CRT $p=0.048$, RCT–CTR $p<0.042$, RCT–TCR $p<0.004$, RCT–TRC $p=0.026$, RCT–RTC $p<0.016$. As with the low resolution subjects, there was a large variance in correction efficacy from subject, but every subject showed the same difference between the corrections. Though all correction orders were significantly better than registration alone, the largest errors occured when slice time correction was applied before RETROICOR (two-tailed, paired t-test: for all orders $p<0.05$) (Fig. 2). Again, the difference between the order of registration and slice-time correction was not significant (two-tailed, paired *t*-test: RTC–TRC $p=0.210$) (Fig. 2). As seen in Fig. 2, the brain regions where the optimal correction orders worked better were in those expected to show physiological fluctuations (i.e. GM and CSF).

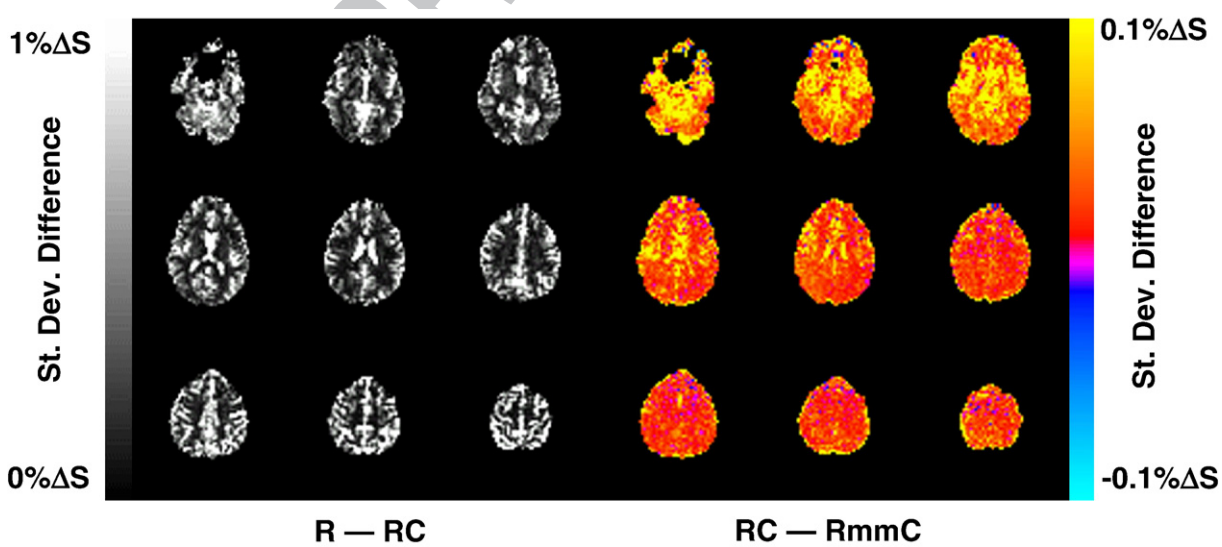

Fig. 4. Comparison between traditional and motion-modified RETROICOR for low-resolution (3.75 mm × 3.75 mm × 5 mm) subject data. The greyscale images on the left represent the difference in temporal standard deviation (i.e. noise reduction) after registration alone (R) and registration followed by RETROICOR (RC). The color images on the right represent additional noise reduction afforded by the motion-modified RETROICOR (RmmC) compared to the traditional RETROICOR (RC) (i.e. RC–RmmC).

Please cite this article as: Jones, T.B., et al., Integration of motion correction and physiological noise regression in fMRI, NeuroImage (2008), doi:10.1016/j.neuroimage.2008.05.019

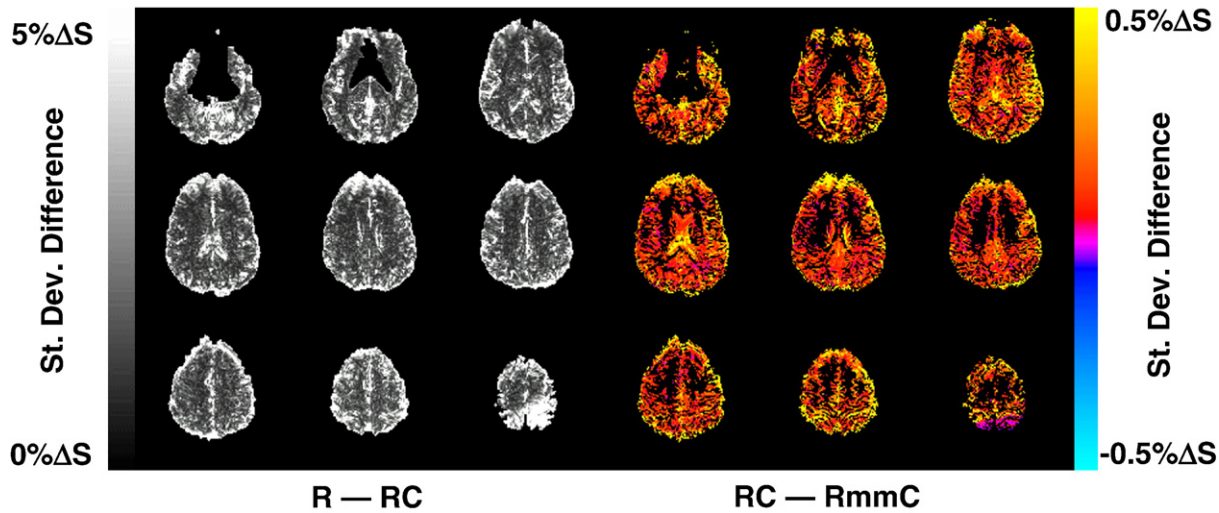

Fig. 5. Comparison between traditional and motion-modified RETROICOR for high-resolution (128×128) subject data. The greyscale images on the left represent the difference in temporal standard deviation (i.e. noise reduction) after registration alone (R) and registration followed by RETROICOR (RC). The color images on the right represent additional noise reduction afforded by the motion-modified RETROICOR (RmmC) compared to the traditional RETROICOR (RC) (i.e. RC–RmmC). Note that to save processing time, the motion-modified RETROICOR (image on right) was performed only in areas with the largest fluctuations (i.e. GM, CSF and large vessels).

Sensitivity of RETROICOR to timing errors introduced by the slice acquisition

There was a noticeable difference in RETROICOR performance between the phase-locked and slice-specific versions as cardiac period variability increased in simulated data (Fig. 3). For a typical cardiac frequency of 1.22 Hz, the performance of the phase-locked version of RETROICOR deteriorates as the cardiac rate variability increases (Fig. 3). Conversely, the slice-corrected version remains effective regardless of cardiac period variability (Fig. 3). Additionally, the effect of not taking individual slice timing into account can be observed in the alternating slice-by-slice performance pattern of the phase-locked version (Fig. 3). This pattern is typical for interleaved slice acquisition when the Fourier regressors from the first slice are used in the nuisance variable regression (NVR).

The difference in performance between the slice-specific and phase-locked versions of RETROICOR observed in simulation was not as prominent in subject data. As seen in Fig. 3, the phase-locked version worked nearly as well as the slice-specific version, the two methods reducing the temporal standard deviation by 22.47% and 22.71%, respectively. Regardless, across the group, the slice-specific version reduced the standard deviation significantly more than the phase-locked version (two-tailed, paired *t*-test: slice-specific — phase-locked $p=0.026$).

Motion-modified RETROICOR

Grey matter and CSF comprise the main areas where the traditional RETROICOR reduces signal variance (Figs. 4 and 5). The motion-modified RETROICOR results in improved noise reduction both at high- and low-resolution, though the effect is smaller in subject data than in simulation (Fig. 6). The motion-modified version of RETROICOR performs better in nearly every voxel in the brain, reducing the temporal noise by up to 8.8% signal change (a reduction of 24.9% compared to the uncorrected temporal noise level). The largest reductions were observed in GM, CSF and at the edges of the brain (Figs. 4 and 5). The increased efficacy of the motion-modified version is particularly noticeable in the frontal region at high resolution, where the relative effects of through-plane motion are larger (Figs. 4 and 5).

In simulation, the motion-modified version of RETROICOR worked markedly better than the traditional method (Figs. 6 and 7). When tested across multiple slices undergoing the same motion as the low-resolution subject data, the motion-modified RETROICOR works 36% better than the traditional RETROICOR (Fig. 6). Fig. 7 shows the effectiveness of the different corrections for increasing amounts of motion (occurring in a linear manner throughout the imaging run), compared to control conditions of no applied corrections ("No corrections") or movement and re-registration of the brain without any simulated cardiac fluctuations ("No fluctuations"). The presence of motion without any physiological fluctuations resulted in an increase in variance, even after volume registration, likely due to interpolation errors. In this simulation, the variance decreased without any applied corrections, since the larger amplitude fluctuations left the slice. The traditional RETROICOR reduces the variance from the simulated physiological noise, but this reduction becomes

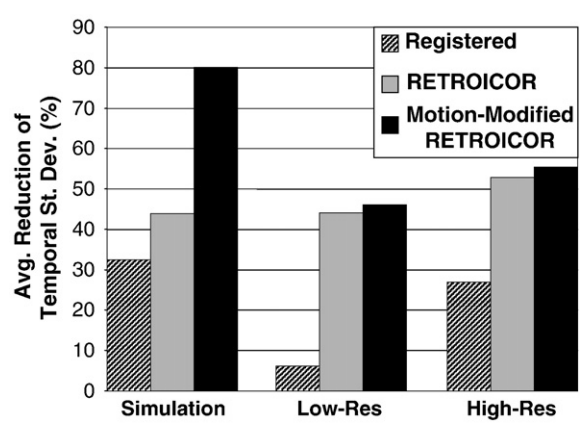

Fig. 6. Performance of the motion-modified RETROICOR in the simulation and subject data. The simulated dataset used the volumetric and motion parameters similar to the low-resolution subject data. Sinusoidal physiological fluctuations were added in a spherical ROI located in the frontal lobe. The average temporal standard deviation represents the average across the frontal ROI in simulation, the whole brain at low resolution and only the GM, CSF and large vessels at high resolution.

Please cite this article as: Jones, T.B., et al., Integration of motion correction and physiological noise regression in fMRI, NeuroImage (2008), doi:10.1016/j.neuroimage.2008.05.019

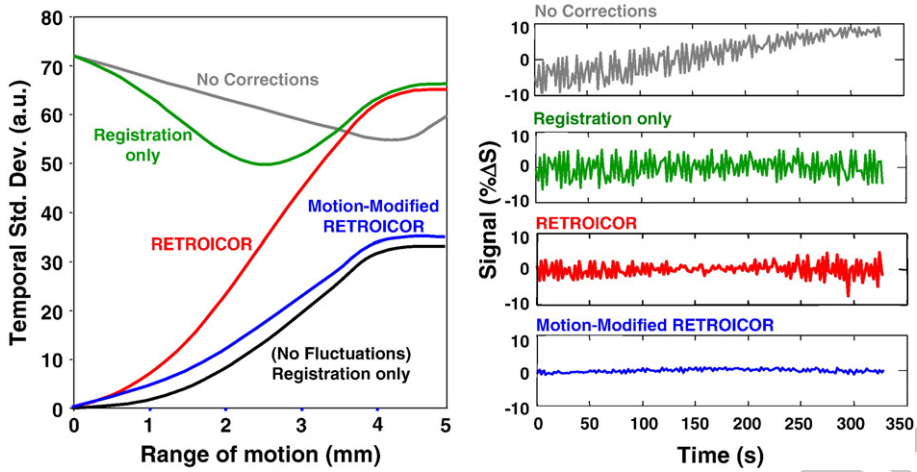

Fig. 7. Simulated corrections for increasing amounts of subject motion, along with representative voxel timecourses. The simulated dataset used volumetric parameters similar to the low-resolution subject data. Sinusoidal physiological fluctuations of varying amplitude from 1.5% to 2.5% (relative to the baseline signal intensity) were added in neighboring slices. The motion consisted of a linear translation in the through-slice direction. The temporal standard deviation before and after various corrections was averaged across the entire slice.

less effective as the amount of motion increases. In contrast, the motion-modified RETROICOR reduces the variance to near that of interpolation errors.

Discussion

There was remarkable consistency across subjects and resolutions with regard to the optimal order of traditional corrections. First performing volume registration, then applying RETROICOR, followed by slice-time correction (RCT) consistently represented the optimal reduction of temporal noise at both high- and low-resolution subject data. While the difference between various orders of corrections was small, it was consistent across voxels and subjects. The smaller relative improvement compared to the simulation may be due to the presence of additional noise. When random noise was added to the simulation, the difference between the various correction orders was reduced (Fig. 1). The increased differentiation in the correction orders at high resolution compared to low resolution could be attributed to the axial slice acquisition in the high-resolution scans, where movement in the sagittal plane (e.g. head nodding), common in fMRI acquisition, would result in relatively larger through-plane motions. Additionally, the high-resolution data would show increased sensitivity to in-plane motion due to smaller voxels. The slice thickness for both high-resolution and low-resolution scans was the same (5 mm), so both should have the same effects of slice-time "mixing" after volume registration.

It should be noted that this particular order (RCT) was optimal for the reduction of temporal noise. The accuracy of the slice-time correction was not assessed, and is likely reduced by the mixing of slice-acquisition times by the volume registration step. The varying response latencies in different voxels due to the varying slice-acquisition times may therefore be modeled more accurately by including some flexibility of the hemodynamic response (e.g. by including the derivative of the response in the model) (Lund et al., 2006). This would also model the variability in the hemodynamic response function across the brain due to factors other than the slice-acquisition times (Aguirre et al., 1998; Handwerker et al., 2004; Saad et al., 1996; Saad et al., 2001). Alternatively, the difference in acquisition times can be accounted for by using a slice-specific design matrix (Worsley et al., 2002). This could be easily incorporated into the motion-modified RETROICOR, which already requires voxel-specific regressors.

According to theory and to our simulations, performing RETROICOR on a slice-by-slice basis (slice-specific) is more accurate than using the regressors of one slice over the whole volume (phase-locked) when the cardiac period is variable. As cardiac period variability increases, misrepresentation of the cardiac phase results in increased errors in the regressors used in RETROICOR. Additionally, in the presence of cardiac period variability, errors become larger in slices acquired at a time further from the slice used in the phase-locked version. In this simulation, we used the acquisition time of the first slice in the volume for the phase-locked version. This is equivalent to assuming that the entire volume was acquired at integer multiples of the imaging repetition time (TR), an assumption that is often made. The errors would be lowered by using the timing of the slice acquired half-way through (in time) of the volume acquisition. Note that when the heart rate is perfectly constant, there is no difference between the slice-specific and phase-locked versions. In real subject data, however, the differences between the slice-specific and phase-locked versions of RETROICOR are minor, even though the variability of the heart rate was similar to that used in the simulation. This suggests that the inaccurate phase information may be overshadowed by other sources of variance. When the data is reshuffled according to phase in the cardiac cycle, for example, one can identify a distinct response function (i.e. a slow variation over the cardiac cycle, time-locked to the heart beat), yet the data still contains significant spread when this variation is removed (Dagli et al., 1999; Glover et al., 2000; Hu et al., 1995).

The motion-modified RETROICOR outlined in this study represents a more accurate model of the physiological noise present in BOLD data. Using a novel approach of scaling the regressors to represent the relative contributions of neighboring slices, the motion-modified version improves on an established method of physiological correction. Simulations indicate that the improvement of the new method is significant. While improvements are not as great in real subject data, the new method performs better than the traditional method in nearly every voxel at both high and low resolutions. It works particularly well in frontal and edge regions known to have increased

Please cite this article as: Jones, T.B., et al., Integration of motion correction and physiological noise regression in fMRI, NeuroImage (2008), doi:10.1016/j.neuroimage.2008.05.019

sensitivity to motion. Furthermore, as with the correction orders analysis, this method would be expected to have an even larger impact on datasets with lower slice thickness and/or larger through-plane movements, representing a potential method for salvaging what otherwise would have been unusable datasets.

A difficulty with the motion-modified version of RETROICOR is that regressors are different for each voxel, a factor that most standard fMRI data analysis packages do not yet handle. Accordingly, regression matrices (e.g. covariance matrices) cannot be pre-computed for the entire volume, resulting in significant computation time for this modified regression. Our first implementation read, processed and wrote each voxel separately, monopolizing computational resources with disk input/output and requiring over 24 h for a single dataset. A new program (3dTfitter), recently developed by Robert Cox, PhD to be part of the AFNI package, allows for a different set of regressors for each voxel. This program is optimized for computational efficiency, requiring only 8 min 24 s to compute the motion-modified RETROICOR on a dataset with 64×64 resolution, TR/TE = 3000 ms/30 ms, 110 images per run, 24 cm FOV, 5 mm slice thickness and axial interleaved slice acquisition on a computer with dual 64-bit AMD Opteron 248 processors running at 2.2 GHz with 2 GB RAM. In comparison, the conventional RETROICOR takes 14.93 s to run on the same machine. While in this study we included only the physiological regressors (since the studies involved resting-state data), task/stimulus regressors or other nuisance regressors could easily be incorporated into this voxel-wise analysis.

As exhibited in the discrepancies between simulations and applications, all three parts of this study indicate that other uncharacterized noise sources remain in BOLD data. One possible source of this inconsistency lies in our model of physiological noise. For example, it may be more accurate to model the cardiac response with a constant impulse response function (IRF) (i.e. using the time to the nearest preceding heart beat), as opposed to stretching it to fit the cardiac period (i.e. using the phase: the time to the nearest preceding heart beat divided by the time between the 2 nearest heart beats), the current method employed in RETROICOR (Deckers et al., 2006). The cardiac IRF may also exhibit great heterogeneity across space, making it more difficult to model; however, doing the regression in a voxel-specific manner should be more accurate on this count. Another confounding factor is variability present in our measurement of when heart beats occur, something of particular concern for our methods as they rely on accurate measurement of cardiac timing. Our peak detection algorithm, which simply considers a heart beat to have occurred when the pulse-oximeter waveform crosses a predefined threshold, could inconsistently reflect the time that the heart contracts. Furthermore, significant variability on the order of tens of milliseconds exists between the pulse-oximeter cardiac waveform and the electrical cardiac waveform, a more accurate measure of cardiac timing information (Foo et al., 2005).

Another discrepancy between our simulations and subject data is the assumption in simulation that motion only occurs between image volumes. Motion during the volume acquisition can result in improper slice alignment, erroneous signal changes, and spin-history effects. Utilizing slice-into-volume registration algorithms could at least partially account for some of these errors (Kim et al., 1999). Motion parameters from such techniques could easily be incorporated into the motion-modified RETROICOR. Additionally, in our simulations motion was applied to lower resolution datasets that were then re-sliced and registered. This resulted in two interpolation steps — one during the application of the motion, and one during the registration, which could lead to additional interpolation errors (smoothing) in the final image. This additional smoothing, however, would be expected to affect all orders of corrections, and both the traditional and motion-modified RETROICOR, and should have minimal effect on the relative performance of the various corrections.

Interpolation errors introduced by volume registration may also corrupt the physiological signal in subject data (Grootoonk et al., 2000). As seen from our simulations (Fig. 7), the improvement afforded by the motion-modified version of RETROICOR is greater for large through-plane movements (>1 mm). Data from a subject exhibiting this level of motion, however, are likely to be significantly corrupted by the motion itself, which standard rigid-body registration algorithms cannot fully correct. However, not all of these residual errors after volume registration can be attributed to interpolation errors. Subject motion, for example, can also result in B_0-field distortions that warp the echo planar images. In addition, T1 spin-history effects are known to have a significant impact on signal variability, and would be aggravated by through-plane motion in interleaved acquisition (Friston et al., 1996). These T1 effects could in principle be modeled and included in the modified RETROICOR correction, although this would require nonlinear fitting approaches if the T1 values are not accurately known for each voxel. Additional improvements may be obtained by modeling the interaction between cardiac and respiratory fluctuations, as done in spinal fMRI by Brooks et al. (2008).

Certainly the best way to deal with all of these effects is to limit subject motion in the first place. This can be accomplished through more careful and consistent head restraint and subject preparation. Another possibility is to employ prospective image correction techniques. Such methods could adjust the imaging parameters and slice positions based on real-time calculations of head position using stereoscopic video positioning systems (Speck et al., 2006; Ward et al., 2000).

Conclusions

This study gives an overview and optimization of current fMRI correction techniques and presents a more accurate model of physiological correction. Using traditional correction routines, performing volume registration before RETROICOR, and not performing traditional slice-time correction before RETROICOR resulted in the greatest reduction of temporal noise. Additional improvements could be attained by implementing a modified version of RETROICOR that takes the effects of volume registration into account. The motion-modified version holds particular promise in use with movement-prone patient populations, at higher resolution, particularly in the *z*-direction, and in studies with specific interests in frontal or edge regions. The methods outlined are of particular interest to functional connectivity studies, where physiological noise can have a significant effect on observed correlations. They may also find application in traditional activation studies by increasing statistical power through noise reduction and noise whitening.

References

Aguirre, G.K., Zarahn, E., D'Esposito, M., 1998. The variability of human, BOLD hemodynamic responses. NeuroImage 8 (4), 360–369.

Please cite this article as: Jones, T.B., et al., Integration of motion correction and physiological noise regression in fMRI, NeuroImage (2008), doi:10.1016/j.neuroimage.2008.05.019

Birn, R.M., Diamond, J.B., Smith, M.A., Bandettini, P.A., 2006. Separating respiratory-variation-related fluctuations from neuronal-activity-related fluctuations in fMRI. NeuroImage 31 (4), 1536–1548.

Biswal, B., Yetkin, F.Z., Haughton, V.M., Hyde, J.S., 1995. Functional connectivity in the motor cortex of resting human brain using echo-planar MRI. Magn. Reson. Med. 34 (4), 537–541.

Brooks, J.C., Beckmann, C.F., Miller, K.L., Wise, R.G., Porro, C.A., Tracey, I., Jenkinson, M., 2008. Physiological noise modelling for spinal functional magnetic resonance imaging studies. NeuroImage 39 (2), 680–692.

Cordes, D., Haughton, V.M., Arfanakis, K., Wendt, G.J., Turski, P.A., Moritz, C.H., Quigley, M.A., Meyerand, M.E., 2000. Mapping functionally related regions of brain with functional connectivity MR imaging. AJNR Am. J. Neuroradiol. 21 (9), 1636–1644.

Cox, R.W., 1996. AFNI: software for analysis and visualization of functional magnetic resonance Neuroimages. Comput. Biomed. Res. 29 (3), 162–173.

Dagli, M.S., Ingeholm, J.E., Haxby, J.V., 1999. Localization of cardiac-induced signal change in fMRI. NeuroImage 9 (4), 407–415.

Deckers, R.H., van Gelderen, P., Ries, M., Barret, O., Duyn, J.H., Ikonomidou, V.N., Fukunaga, M., Glover, G.H., de Zwart, J.A., 2006. An adaptive filter for suppression of cardiac and respiratory noise in MRI time series data. NeuroImage 33 (4), 1072–1081.

Foo, J.Y., Wilson, S.J., Dakin, C., Williams, G., Harris, M.A., Cooper, D., 2005. Variability in time delay between two models of pulse oximeters for deriving the photoplethysmographic signals. Physiol. Meas. 26 (4), 531–544.

Friston, K.J., Williams, S., Howard, R., Frackowiak, R.S., Turner, R., 1996. Movement-related effects in fMRI time-series. Magn. Reson. Med. 35 (3), 346–355.

Glover, G.H., Li, T.Q., Ress, D., 2000. Image-based method for retrospective correction of physiological motion effects in fMRI: RETROICOR. Magn. Reson. Med. 44 (1), 162–167.

Grootoonk, S., Hutton, C., Ashburner, J., Howseman, A.M., Josephs, O., Rees, G., Friston, K.J., Turner, R., 2000. Characterization and correction of interpolation effects in the realignment of fMRI time series. NeuroImage 11 (1), 49–57.

Handwerker, D.A., Ollinger, J.M., D'Esposito, M., 2004. Variation of BOLD hemodynamic responses across subjects and brain regions and their effects on statistical analyses. NeuroImage 21 (4), 1639–1651.

Hu, X., Le, T.H., Parrish, T., Erhard, P., 1995. Retrospective estimation and correction of physiological fluctuation in functional MRI. Magn. Reson. Med. 34, 201–212.

Kim, B., Boes, J.L., Bland, P.H., Chenevert, T.L., Meyer, C.R., 1999. Motion correction in fMRI via registration of individual slices into an anatomical volume. Magn. Reson. Med. 41 (5), 964–972.

Kruger, G., Glover, G.H., 2001. Physiological noise in oxygenation-sensitive magnetic resonance imaging. Magn. Reson. Med. 46 (4), 631–637.

Lowe, M.J., Mock, B.J., Sorenson, J.A., 1998. Functional connectivity in single and multislice echoplanar imaging using resting-state fluctuations. NeuroImage 7 (2), 119–132.

Lund, T.E., 2001. fcMRI-mapping functional connectivity or correlating cardiac-induced noise? Magn. Reson. Med. 46 (3), 628–629.

Lund, T.E., Madsen, K.H., Sidaros, K., Luo, W.L., Nichols, T.E., 2006. Non-white noise in fMRI: does modelling have an impact? NeuroImage 29 (1), 54–66.

Saad, Z.S., Ropella, K.M., Carman, G.J., DeYoe, E.A., 1996. Temporal phase variation of FMR signals in vasculature versus parenchyma. ~~Proceedings of ISMRM 4th Annual Meeting. New York~~ Q2

Saad, Z.S., Ropella, K.M., Cox, R.W., DeYoe, E.A., 2001. Analysis and use of fMRI response delays. Hum. Brain Mapp. 13 (2), 74–93.

Speck, O., Hennig, J., Zaitsev, M., 2006. Prospective real-time slice-by-slice motion correction for fMRI in freely moving subjects. Magma 19 (2), 55–61.

Ward, H.A., Riederer, S.J., Grimm, R.C., Ehman, R.L., Felmlee, J.P., Jack Jr, C.R., 2000. Prospective multiaxial motion correction for fMRI. Magn. Reson. Med. 43 (3), 459–469.

Weisskoff, R.M., Baker, J., Belliveau, J., Davis, T.L., Kwong, K.K., Cohen, M.S., Rosen, B.R., 1993. Power spectrum analysis of functionally weighted MR data: what's in the noise? International Society of Magnetic Resonance in Medicine.

Wise, R.G., Ide, K., Poulin, M.J., Tracey, I., 2004. Resting fluctuations in arterial carbon dioxide induce significant low frequency variations in BOLD signal. NeuroImage 21 (4), 1652–1664.

Worsley, K.J., Liao, C.H., Aston, J., Petre, V., Duncan, G.H., Morales, F., Evans, A.C., 2002. A general statistical analysis for fMRI data. NeuroImage 15 (1), 1–15.

Please cite this article as: Jones, T.B., et al., Integration of motion correction and physiological noise regression in fMRI, NeuroImage (2008), doi:10.1016/j.neuroimage.2008.05.019